The Burkholderia cenocepacia peptidoglycan-associated lipoprotein is involved in epithelial cell attachment and elicitation of inflammation

Dennehy, R., Romano, M., Ruggiero, A., Mohamed, Y. F., Dignam, S. L., Mujica Troncoso, C., Callagham, M., Valvano, M. A., Berisio, R., & McClean, S. (2017). The Burkholderia cenocepacia peptidoglycan-associated lipoprotein is involved in epithelial cell attachment and elicitation of inflammation. *Cellular Microbiology*, *19*(5), [e12691]. https://doi.org/10.1111/cmi.12691

Published in:
Cellular Microbiology

Document Version:
Peer reviewed version

Queen's University Belfast - Research Portal:
Link to publication record in Queen's University Belfast Research Portal

The *Burkholderia cenocepacia* peptidoglycan-associated lipoprotein is involved in epithelial cell attachment and elicitation of inflammation

Ruth Dennehy[1#], Maria Romano[2], Alessia Ruggiero[2], Yasmine F. Mohamed[3,4], Simon Dignam[1], Cristóbal Mujica Troncoso [3], Máire Callaghan[1], Miguel A. Valvano[3], Rita Berisio[2], Siobhán McClean[1]*

[1] Centre of Microbial Host Interactions, Institute of Technology Tallaght, Old Blessington Road, Dublin 24.
[2] Institute of Biostructures and Bioimaging, National Research Council, Via Mezzocannone 16, I-80134 Naples, Italy;
[3] Centre for Experimental Medicine, Queen's University, Belfast, BT9 7BL, UK
[4] Department of Microbiology, Faculty of Pharmacy, Alexandria University, Egypt

*To whom correspondence should be addressed: Dr Siobhán McClean, Centre of Microbial Host Interactions, Institute of Technology Tallaght, Old Blessington Road, Dublin 24; Email: siobhan.mcclean@ittdublin.ie
Phone: +353-1-4042794

Keywords:
Peptidoglycan associated lipoprotein; cystic fibrosis; host cell attachment; inflammation; pathogen associated molecular patterns.

Running Title: Pal mediates host cell attachment

Cellular Microbiology

[#] Current address: Pfizer Ireland, Dublin 22, Ireland

Summary

The *Burkholderia cepacia* complex (Bcc) is a group of Gram-negative opportunistic pathogens causing infections in people with cystic fibrosis (CF). Bcc are highly antibiotic resistant, making conventional antibiotic treatment problematic. The identification of novel targets for anti-virulence therapies should improve therapeutic options for infected CF patients. We previously identified that the peptidoglycan-associated lipoprotein (Pal) was immunogenic in Bcc infected CF patients; however, its role in Bcc pathogenesis is unknown. The virulence of a *pal* deletion mutant (Δ*pal*) in *Galleria mellonella* was 88-fold reduced ($p<0.001$) compared to wild-type. The lipopolysaccharide profiles of wild-type and Δ*pal* were identical, indicating no involvement of Pal in O-antigen transport. However, Δ*pal* was more susceptible to polymyxin B. Structural elucidation by X-ray crystallography and calorimetry demonstrated that Pal binds peptidoglycan fragments. Δ*pal* showed a 1.5-fold reduced stimulation of IL-8 in CF epithelial cells relative to wild-type ($p<0.001$), demonstrating that Pal is a significant driver of inflammation. The Δ*pal* mutant had reduced binding to CFBE41o$^-$ cells, but adhesion of Pal-expressing recombinant *E. coli* to CFBE41o$^-$ cells was enhanced compared to wild-type *E. coli*, confirming that Pal plays a direct role in host cell attachment. Overall, Bcc Pal mediates host cell attachment and stimulation of cytokine secretion, contributing to Bcc pathogenesis.

Introduction

The *Burkholderia cepacia* complex (Bcc) is a group of closely related Gram-negative bacteria causing opportunistic chronic infections in people with cystic fibrosis (CF). The complex currently comprises 20 species, the majority of which are highly resistant to different classes of antibiotics (Peeters et al., 2013, De Smet et al., 2015). While all species can potentially cause airway infections in people with CF, the most clinically relevant are *B. multivorans* and *B. cenocepacia* (Drevinek and Mahenthiralingam, 2010). Further, a subset of CF patients infected with Bcc can develop an aggressive infection with septicaemia and rapid decline in lung function, referred to as cepacia syndrome (Isles et al., 1984). Since Bcc bacteria are highly resistant to most clinically used antibiotics there is a need for alternative therapies. Identifying, understanding, and targeting specific virulence determinants may unravel novel means to control Bcc infection.

We have recently identified immunoreactive proteins expressed by *B. cenocepacia* and *B. multivorans* during human infection using an immunoproteomics approach (Shinoy et al., 2013). The peptidoglycan-associated lipoprotein (Pal, GI:357936457), encoded by BCAL3204 was among the immunogenic proteins that were consistently identified in *B. multivorans* and *B. cenocepacia.* Pal from both species generated pronounced antibody responses in Bcc infected patients. Lipoproteins play roles in the pathogenesis of various bacterial species (McClean, 2012), as they are involved in signal transduction, conjugation and nutrient uptake, and also play a role in antibiotic resistance, transport, and extra-cytoplasmic folding of proteins. Lipoproteins also facilitate bacterial adhesion, invasion, colonization, immunomodulation and evasion of host defence, as recently reviewed (Kovacs-Simon et al., 2011). For example, a

reduction in fibronectin and laminin binding was demonstrated for *Streptococcus pyogenes* Lsp mutants that were defective in lipoprotein release, with the mutant showing reduced levels of adhesion and internalization (Elsner et al., 2002). Lipoproteins were also classed as pathogen-associated molecular patterns (PAMPs) which play a role in modulating the host immune response and are recognized by TLR-2 receptors (Godlewska et al., 2009). Pal is a component of the Tol/Pal complex and the genes encoding Tol and Pal proteins comprise two adjacent operons in *E. coli* and in other bacterial species. The Tol/Pal complex is required for maintaining cell wall integrity (Lazzaroni et al., 1999, Rodriguez-Herva et al., 1996) and for regulation and co-ordination of outer-membrane invagination during cell constriction in *E. coli* (Gray et al., 2015, Gerding et al., 2007). Tol/Pal proteins play a role in the transport of LPS subunits, including the O-antigen region, to the outer membrane (Vines et al., 2005, Gaspar et al., 2000). Pal expressed by Gram-negative bacteria possesses a region with conserved surface residues that forms a binding pocket for the meso-diaminopimelate (m-DAP) residue of peptidoglycan (Parsons et al., 2006). Pal is anchored in the outer membrane and interacts independently with OmpA and Lpp envelope proteins (Godlewska et al., 2009). Recently, it was shown that between 10 to 20% of *E. coli* cells express Pal on their surface (Michel et al., 2015). The non-typeable *Haemophilus influenzae* Pal homologue P6 also has a dual orientation, being exposed infrequently on the surface, but predominantly oriented towards the periplasmic space (Michel et al., 2013). Pal can be secreted into the extracellular environment or the bloodstream during infection, contributing to septic shock (Hellman et al., 2002). *E. coli* Pal is released into human serum in tight association with LPS, inducing TLR2-mediated cytokine production by macrophages. Pal and LPS synergistically activate macrophages indicating that Pal may play an important

role in inflammation and the pathogenesis of sepsis (Liang et al., 2005). Despite considerable studies in other organisms, the role of Pal in Bcc pathogenesis was not investigated previously. The strong anti-Pal immunogenic response in Bcc colonised CF patients (Shinoy et al., 2013) demonstrates that the protein interacts with the human immune system and suggests a role in pathogenesis. Here, we demonstrate that Bcc Pal is structurally similar to *E. coli* Pal, possessing the conserved peptidoglycan-binding site. We also developed a targeted Pal deletion mutant in *B. cenocepacia* and show that Pal plays a role in virulence in an acute infection model, it is a potent driver of IL-8 secretion, and mediates adhesion to lung epithelial cells.

RESULTS

Pal is required for pathogenicity in the Galleria mellonella *infection model*

The Δ*pal* mutant and *B. cenocepacia* K56-2 wild-type strains had comparable growth curves in LB with doubling times of 80 and 90 min respectively. To investigate if Pal has a role in virulence, the survival of the *G. mellonella* larvae was evaluated following infection with the Δ*pal* deletion mutant in comparison with K56-2. While K56-2 was highly lethal to *G. mellonella* (LD_{50} of 1.66 $\pm$ 1.91 at 48 h), Δ*pal* demonstrated substantially attenuated virulence (88-fold increase in LD50 of 145.5 $\pm$ 6; $p<0.001$). The virulence phenotype was partially complemented when the *pal* gene was encoded on a pDA-12 plasmid (LD_{50} of 40 $\pm$ 5.7) suggesting that the virulence phenotype may be gene dosage dependent and highlights the complexity of virulence in this model. Purified recombinant Pal_{Bc} did not affect larval survival, with 100% of larvae surviving after 72 h exposure to up to 3 μg (maximum dose allowable based on

injection volume) of purified recombinant protein, indicating that this amount of pure Pal is not toxic to the larvae.

Larvae injected with cell free supernatant (CFS) from Δ*pal* showed reduced survival (60% survival at 72 h) relative to those injected with CFS from wild-type (80% survival at 72 h), ($P<0.0001$) (Fig. 1). When *pal* gene expression was reconstituted chromosomally in the Δ*pal* mutant, the CFS from complemented Δ*pal*(*pal*$^+$) strain did not affect survival at 72 h. We conclude that this phenotype reflects impaired outer membrane integrity of Δ*pal*, which allows release of periplasmic proteins and outer membrane vesicles to the external milieu contributing to the enhanced toxicity of the supernatant fraction from this strain. Impaired outer membrane integrity was confirmed by measuring the uptake of the fluorescent dye H33342. A 1.4-fold difference in dye uptake was apparent within 30 min by the Δ*pal* mutant over wild-type K56-2 cells, while this difference disappeared in the complemented Δ*pal*(*pal*$^+$) strain and this was sustained for over 90 min ($P<0.0001$, Fig. 1C).

Pal does not affect LPS phenotype, but is involved in polymyxin resistance

LPS was isolated from wild-type and mutant strains to assess if the Δ*pal* mutant had a defect in O-antigen expression. Comparison of LPS extracts from mutant and wild-type on 15 % acrylamide gels showed no discernible difference in the LPS electrophoretotypes between the Δ*pal* mutant and wild-type K56-2 (Fig. 2A). This was confirmed by mass spectrometry of the lipid A from wild-type K56-2 and the Δ*pal* mutant (Fig. 2B) and indicates that the decreased virulence of the mutant was independent of LPS composition. As polymyxin B targets LPS components, the sensitivity of Δ*pal* to polymyxin B was also examined. Wild-type K56-2 was highly

resistant to polymyxin B on Mueller Hinton agar (MIC 96 μg/ml), but Δ*pal* was three-fold more sensitive (MIC of 32 μg/ml) (Fig. S1). Polymyxin B resistance was restored in the complemented strain Δ*pal*(*pal*$^{+}$), confirming that polymyxin susceptibility was due to the loss of Pal. These results suggest that despite the lack of apparent differences in LPS the Δ*pal* mutant has compromised outer membrane permeability. In comparison, there was no difference in susceptibility to either levofloxacin (not shown) or meropenem between the wild-type and Δ*pal* mutant (Fig. S1).

B. cenocepacia *Pal is a lipoprotein with a conserved peptidoglycan-binding site*

B. cenocepacia Pal (Pal_{Bc}) is a predicted lipoprotein. Consistent with this, its sequence has a hydrophobic N-terminal lipoprotein signal peptide followed by the LAAC lipobox motif, consistent with proteolytic processing by signal peptidase II during translocation across the cytoplasmic membrane (cleavage site between LAA-C, Fig. 3A). Electron spray MS analysis of purified His-tag Pal_{Bc} showed it has a mass of 22820 $\pm$5 Da, equivalent to the theoretical mass of Pal_{Bc} with poly-His and the Xpress epitope (Fig. S2, S3). Pal_{Bc} co-purifies with acylated forms, with masses consistent with the palmitoylated (23520 Da), myristoylated (23460 Da) and laurylated forms (23408 Da) all having a DAP residue (190.2). These were identified in the spectrum with relative abundances as determined by peak height ratios of 5:1:1:0.5 (Fig. S3). This is consistent with the recombinant Pal_{Bc} being lipidated at the lipobox in the *E. coli* BL21Star cells and is expressed as a lipoprotein.

As predicted by the Pfam database, Pal_{Bc} also contains an OmpA domain (Fig. 3). Based on these analyses and on secondary structure predictions, we cloned and expressed a truncated form of Pal containing residues 51 to 170 (Pal_{51-170}), which was

amenable to crystallization. Pal_{51-170} was monomeric in solution, as evidenced by both size exclusion chromatography and dynamic light scattering (Fig. 3B and C). Circular dichroism spectra show that Pal_{51-170} adopts a α-β-conformation (Fig. 3D). Also, thermal unfolding curves, achieved by following the CD signal at 222 nm as a function of temperature, indicate a stable structure, with melting temperature Tm=48°C (Fig. 3E). Crystals of Pal_{51-170} suitable for X-ray diffraction were obtained using vapour diffusion techniques and belonged to the hexagonal space group $P3_2$. The structure was solved by molecular replacement and refined at 2.0 Å (Table 3). The structure includes two molecules in the asymmetric unit, with close structural similarity (r.m.s.d. 0.2 Å upon superposition of Cα atoms 52-170). Consistent with CD data, the overall structure of each molecule showed a α-β sandwich fold, organized in a helix-strand-helix topology (Fig. 4A). The analysis of the protein surface revealed a deep cavity (located close to the N-terminal ends of the α-helix α2) whose rear wall is contributed by the side chain of Arg120 (Fig. 4B). Surface conservation computation, carried out with ConSurf (Goldenberg et al., 2009), showed that the residues forming the cavity, namely Asp-71, Asp-105, Gly-106, Tyr-112, Asn-113, Arg-120, are highly conserved (Fig. 4C). This conservation indicates a functional role for this surface region and agrees with the finding that mutants of Asp-197 and Arg-217 in the OmpA-like MotB of *E. coli* (corresponding to Asp-105 and Arg-120 in Pal_{51-170}, respectively) are non-functional *in vivo* (Blair et al., 1991).

Analysis of electron density maps showed density blobs which were not associated with protein residues in the Pal_{51-170} crystals and not compatible with any molecules from the crystallization medium. This density was interpreted as belonging to a muropeptide fragment; probably a fragment of the *E. coli* peptidoglycan bound to the

protein upon lysis and carried through the purification process. Likely, Pal_{51-170} recognizes common features between its physiological substrate in *B. cenocepacia* and a muropeptide of *E. coli*, as both species produce DAP-type peptidoglycan. Based on the shape and size of electron density, a DAP molecule was built in each cavity of the two molecules in the asymmetric unit (Fig. 4D). In each molecule, DAP is deeply immersed in the identified cavity (Fig. S4) having its carboxylate engaging the guanidinium group of Arg-120 in a bidentate salt bridge. This carboxylate also forms hydrogen bonds to the main-chain amide protons of Asp-105. Nζ of DAP is H-bonded to the side chain of Asp-105 and the main chain carbonyl oxygen of Arg-106 (Fig. 4D). Hydrophobic interactions also involve Phe-72 and Arg-106, Leu-116, all highly conserved residues. The maps show further density, not interpretable likely due to high flexibility of the bound muropeptide. The binding mode of DAP to Pal_{51-170} resembles that of OmpA of *E. coli* (Park et al., 2012), with a similar structural organization of interacting residues (Fig. S5).

The ability of Pal_{51-170} to bind muropeptides was confirmed by Isothermal Titration Calorimetry (ITC) (Fig. 5 A and B). Binding isotherms for the interaction of Pal_{51-170} with the muropeptide fragment (iE-DAP, measured at pH 7.5) were characterized by exothermic heats of binding which decreased in magnitude with successive injections of ligand until saturation was achieved. These data indicate a moderate protein-ligand binding affinity, with K_D of 27.4 (±7.4) μM and ΔH of 4.3 (±0.4) Kcal/mol, respectively.

Pal_{Bc} stimulates a potent pro-inflammatory response

We previously showed that Pal expressed by *B. multivorans* and *B. cenocepacia*

stimulate a strong antibody response in infected CF patients (Shinoy et al., 2013). To determine if Pal also contributes to pro-inflammatory responses, we examined the secretion of cytokines from CF lung epithelial cells (CFBE41o$^-$) after infection with Δ*pal* or wild-type K56-2 strains. While infection with K56-2 strain induced potent stimulation of IL-8 and IL-6 secretion, infection with Δ*pal* resulted in reduced IL-8 secretion (1.5-fold, $p<0.001$) with no difference in IL-6 secretion (Fig. 6). These results indicate Pal contributes to IL-8 stimulation, as expected from a lipoprotein. Weak but comparable secretion of IL-4 and Interferon-γ were observed for wild-type and mutant strains, and no differences were found in the secretion of IL-10, IL12p70, IL-13, IL-1β, IL-2 or TNFα. Secretion of IL-8 by CFBE41o$^-$ cells exposed to purified, endotoxin-free Pal_{Bc} increased in a concentration dependent manner, in comparison to the medium control samples (Fig. 6C), confirming that the observed reduced secretion of IL-8 following infection with the Δ*pal* mutant was a direct effect of the absence of Pal. Indeed, 50 μg/ml $Pal_{Bc,}$ stimulated comparable levels of IL-8 relative to the levels from cells incubated with purified LPS (100 μg/ml) from *B. cenocepacia* K56-2 (Fig. 6C), highlighting the potency of Pal_{Bc} in the chemokine response. Although the Δ*pal* mutant did not alter IL-6 secretion, the levels of this cytokine increased 3-fold in response to 100 μg/ml Pal_{Bc} compared to the MEM control (Fig. 6D). Pal_{Bc} was not as effective in stimulation of IL-6 secretion relative to LPS at the same concentration (100 μg/ml), Pal_{Bc} induced IL-6 levels of 285 pg/ml for Pal_{Bc} compared with 516 pg/ml for LPS. Pal_{Bc} did not stimulate secretion of any other cytokines in the panel, IFNγ, IL-10, IL12p70, IL-13, IL-1β, IL-2, IL-4 or TNFα, at concentrations up to 100 μg/ml.

*Pal is involved in attachment to human lung epithelial cells***.**

The attachment of bacteria to host cells is an important step in the colonization process and many immunogenic proteins stimulate the host response via direct interaction with the host epithelium. The C-terminus of Pal shares homology with OmpA proteins which were associated with the host cell attachment of several pathogens (McClean, 2012). The attachment of the Δ*pal* mutant to CFBE41o$^-$ lung epithelial cells was compared to the wild-type K56-2 strain to determine if Pal is involved in the attachment of Bcc to lung cells. We used two independent methods, cell lysis and subsequent plating to determine the CFU/ml attached and confocal microscopy. There was a 2.5-fold reduction in binding of the Δ*pal* mutant relative to K56-2 cells ($p=0.0189$), with host cell attachment being reduced to that of the negative control, *E. coli* strain NCIB9485. This was confirmed by confocal immunofluorescence microscopy, which showed a 34% reduction in attachment of the Δ*pal* mutant relative to wild-type K56-2 (Fig. 7, $p=0.0462$). Adhesion was restored to wild-type levels in the Δ*pal*(*pal*$^+$) complemented strain (Fig. 7).

To further evaluate the role of Pal in host cell attachment and to investigate whether the protein plays a direct role in cellular attachment recombinant *E. coli* BL21 cells expressing Pal_{Bc} under β-D-1-thiogalactopyranoside (IPTG) induction (Kim et al., 2010, Plesa et al., 2004) were examined for their ability to bind to CFBE41o$^-$ cells, relative to *E. coli* BL21 cells and again quantified using confocal microscopy (Fig. 8A). *E. coli* BL21 cells bind poorly to CFBE41o$^-$ cells, as expected, with two bacteria being attached per 100 epithelial cells (Fig. 8B). Attachment of BL21 cells induced to express Pal_{Bc} showed an increase in attachment to CFBE41o$^-$ cells relative to control BL21 cells ($p<0.0001$), suggesting that Pal interacts directly with the lung epithelial cells, rather than indirectly being involved in attachment via regulation of

other proteins.

Discussion

The Tol/Pal system was extensively studied in *E. coli* and is associated with various physiological processes in *E. coli* including cell wall integrity and constriction of the outer membrane. The Pal C-terminus also shares high homology with OmpA, which is associated with host cell attachment of many pathogens (McClean, 2012, De Mot and Vanderleyden, 1994). TolB and Pal are poorly conserved proteins, although ubiquitous across Gram-negative organisms; however, they are conserved among Bcc species (Plesa et al., 2004). Pal is essential for survival and pathogenesis in other bacteria, although its role in virulence was not clearly defined (Godlewska et al., 2009). We have previously shown that Pal is immunogenic in Bcc colonised CF patients (Shinoy et al., 2013), but little was know about the role of Pal in Bcc. In this study, we have demonstrated that the Pal protein from *B. cenocepacia* plays a role in virulence and mediates host cell attachment. In addition, we have demonstrated that Pal_{Bc} stimulates IL-8 secretion.

The crystal structure of the OmpA-like domain of Pal_{Bc} revealed strong structural similarities with Pal proteins from *B. pseudomallei* and *E. coli*, which form a characteristic α-β sandwich fold (Gourlay et al., 2013). Further, the Pal_{Bc} structure confirmed its potential to bind peptidoglycan, consistent with the conservation of specific residues that contribute to a deep cavity where the DAP moiety is located. It is likely that peptidoglycan binding plays an important role in anchoring of the outer membrane to the bacterial cell wall and contributing to maintain cell envelope integrity (Park et al., 2012) and may also limit the lateral diffusion of OmpA proteins in outer membranes (Verhoeven et al., 2013, Winther et al., 2009).

Mutations defective in Tol/Pal proteins are not always lethal suggesting that other outer membrane proteins may act as substitutes (Godlewska et al., 2009). Mutations typically result in hypersensitivity to detergents and/or antibiotics (Cascales et al., 2002) and disruption of cell-envelope integrity (Rodriguez-Herva et al., 1996), suggesting a role for these proteins in maintaining structure and function of the cell envelope. Consistent with this notion, Pal_{Bc} also has a role in maintaining membrane integrity as determined by the increase in permeability to H33342. In addition the enhanced lethality of cell free supernatant from the Bcc Δ*pal* strain to *G. mellonella* compared with WT is also suggestive of release of virulence factors and/or inflammatory mediators in the mutant. Further, the enhanced sensitivity of Δ*pal* to the membrane-acting antibiotic polymyxin also denotes enhanced outer membrane permeability. Polymyxin binds to LPS, allowing its hydrophobic tail to disrupt both bacterial membranes. Given that the permeability of the mutant is impaired due to the lack of Pal, it is reasonable to assume the mutant would also be more susceptible to the detergent action of the hydrophobic tail. In contrast, no alteration in meropenem susceptibility was observed. This is expected, as meropenem inhibits peptidoglycan synthesis and although Pal binds to peptidoglycan, the synthesis of the peptidoglycan layer should remain unimpaired in the Pal mutant and consequently both mutant and wild-type show similar susceptibilities. Despite reports that the Tol/Pal system has a role in the biogenesis and transport of LPS components in *E. coli* (Gaspar et al., 2000, Vines et al., 2005), Pal_{Bc} does not appear to be required for LPS transport, as the Δ*pal* mutant and wild-type showed comparable LPS profiles. Given the high degree of modularity that exists in Tol/Pal complex, it is plausible that those individual components in the complex are replaced across evolution and that functional roles associated with one

member of the complex in a bacterial species, may be carried out by another member of the Tol/Pal complex in other bacteria.

OmpA-like proteins were associated with a variety of virulence factors (Prasadarao et al., 1996, Sukumaran et al., 2003, Torres and Kaper, 2003). Consistent with these studies, we have shown that the Pal mutant reduced virulence in *G. mellonella* by 88-fold. It is still unknown how Bcc kills the larvae; however, it was shown that virulence in *G. mellonella* correlates well with survival of Bcc infected mice (Seed and Dennis, 2008). It is difficult to postulate how Pal may play a role in larval death, but the progress of infection was accompanied by increased melanisation, which is indicative of larval immune response. Lethality may be due to an overwhelming immune response to infection, and related to the potency of Pal in stimulating pro-inflammatory response in epithelial cells. Exposure of CF cells to the Δ*pal* mutant showed that Pal_{Bc} is a potent stimulator of the IL-8 chemokine. Considering all the potential PAMPs expressed on the surface of the wild-type strain K56-2 (LPS, flagellin, outer membrane proteins, other lipoproteins) (Hanuszkiewicz et al., 2014, Ortega et al., 2005), the fact that the Δ*pal* mutant reduces IL-8 secretion by 33% demonstrates Pal is a key driver of Bcc-induced IL-8 secretion in CF lung epithelial cells. IL-8 stimulation was confirmed with Pal_{Bc}, which stimulated comparable levels of IL-8 to LPS. IL-8 is a chemotactic cytokine and is particularly important in CF as inflammation is a neutrophil-dominated process in the CF lung. The substantially impaired IL-8 secretion elicited by the Δ*pal* mutant indicates that Pal is a significant contributor to the overall inflammatory response in the CF lung. Pal_{Bc} also stimulated IL-6 secretion, albeit to a lesser degree than IL-8. The Δ*pal* mutant did not have any impact on IL-6 secretion of the K56-2 strain, highlighting that while Pal can stimulate IL-6 secretion, other PAMPs in *B. cenocepacia* are more

predominant stimulators of IL-6 and the absence of Pal in the mutant was compensated for by other PAMPs. Despite that Pal, consistent with other bacterial lipoproteins, most likely activates TLR2 (Zhu et al., 2007, Liang et al., 2005, Berenson et al., 2005), we used LPS, a TLR-4 activator, as a positive control, as we have shown it is a potent stimulator of IL-8 and IL-6 in CFBE41o$^-$ cells (Kaza et al., 2010). The host response to Pal_{Bc} requires more investigation to further examine its role in inflammation and the signalling pathways involved in the response to Pal.

Pal is generally regarded as an outer membrane periplasmic protein and was not previously associated with a role in host cell attachment. We clearly show that Bcc Pal is involved in the attachment of Bcc to lung epithelial cells, with the Δ*pal* mutant cells showing reduced ability to bind to lung epithelial cells, which was reversed in the complemented strain. Furthermore, recombinant *E. coli* expressing the complete Pal_{Bc} transcript showed enhanced attachment to CF lung cells, indicating that Bcc Pal can directly mediate the attachment of Bcc to the host epithelium. MS analysis showed that Pal_{Bc} is expressed in its lipidated form and while it was purified from cell lysates via its His-tag, a quantity of the expressed protein is likely to be cleaved following lipidation and transported through the inner membrane. Other lipoproteins are involved in facilitating host cell adhesion, for example an outer membrane lipoprotein, from *Moraxella catarrhalis*, which shares 58% homology with *P. aeruginosa* LppL, is important in the attachment of *M. catarrhalis* to human respiratory tract cells (de Vries et al., 2013). Pal has a conserved surface-exposed epitope in *H. ducreyi* (Spinola et al., 1994) and more recently was reported to be surface expressed in a subpopulation of *E. coli* cells (Michel et al., 2015). Given the similarities between Bcc and *E. coli* Pal shown here, it is highly likely that Pal can also be partially expressed at the surface of Bcc cells, mediating the direct interaction

between Bcc and host epithelial cells. The membrane localisation of Pal_{Bc} would need to be confirmed experimentally and is the basis of future work.

Pal was among a group of genes that were induced *in vivo* in a chronic respiratory infection model, suggesting that it contributed to bacterial adaptation and survival in the lungs (O'Grady and Sokol, 2011). We have recently shown that attachment to CF epithelial cells was enhanced over time of chronic colonisation in a series of sequential clinical *B. cenocepacia* isolates (Cullen et al., accepted manuscript), therefore the observed induction of Pal in the chronic rat infection model complements our findings as it suggests that Pal may contribute to the enhanced host cell attachment observed in the clinical chronic infection isolates and its expression may contribute to successful colonization of the host. The involvement in host cell attachment is also consistent with findings that a lipoprotein, which subsequently showed 95.8% identity to the Pal encoded by BCAL3204, was the immunodominant antigen in Bcc infected mice (Makidon et al., 2010, O'Grady and Sokol, 2011).

In summary, this study demonstrates that Pal_{Bc} is structurally similar to Pal proteins in other Gram-negative bacteria, is involved in peptidoglycan binding and can mediate host cell attachment to epithelial cells. More importantly, Pal_{Bc} is a strong stimulator of IL-8 secretion, becoming a major contributor to inflammation in the lung with comparable potency to LPS.

Experimental Procedures

Bacterial strains

B. cenocepacia K56-2 was obtained from the BCCM/ LMG, University of Ghent, Belgium and was routinely plated onto *Burkholderia* cepacia selective agar (BCSA) (Henry et al., 1997). Bacteria were grown in Luria Bertani (LB) broth at 37 °C with orbital agitation (150 rpm). The growth rate of wild type and mutant strains was determined in LB broth at 37 °C over 7 h. Samples were taken every 30 min and plated on LB agar. Colonies were counted and plotted against time of sampling to determine the generation time.

Culturing epithelial cells

The CFBE41o$^-$ lung epithelial cell line, which is homozygous for the CFTR ΔF508 mutation, the most commonly inherited CF mutation, was a gift from Dr. Dieter Gruenert (UCSF California). CFBE41o$^-$ cells were maintained in MEM medium with 10 % (v/v) FBS, 1 % penicillin/streptomycin, 1 % L-glutamine and 1 % non-essential amino acids and incubated in 5 % CO_2 environment at 37 °C.

Mutagenesis of B. cenocepacia K56-2 and complementation

Unmarked and non polar mutations were performed by the protocol of Flannagan *et al*. (Flannagan et al., 2008). The amplicons to construct the mutagenic plasmid were digested with EcoRI-HindIII and HindIII-NheI, respectively, and cloned into pGPI-SceI-2 digested with EcoRI and NheI. Once introduced by conjugation into *B. cenocepacia* K56-2, the mutagenic plasmid integrates into the chromosome, giving rise to trimethoprim-resistant exconjugants. A second plasmid, pDAISce-I, encoding the I-SceI endonuclease was then introduced by conjugation resulting in double-

strand breaks in the chromosome at the Sce-I recognition site. The deletion of *pal* (BCAL3204) was first analyzed by PCR and then confirmed by DNA sequencing. To complement *B. cenocepacia* K56-2 Δ*pal*, wild-type *pal* was PCR amplified from *B. cenocepacia* K56-2 (see primers in Table 2). The resulting amplicon was digested with NdeI and XbaI and ligated into a similarly digested pMH447 vector. The complementation plasmid was introduced into the mutant by conjugation. Once transferred into the target mutant strain the complementation vector integrates into the genome at aminoglycoside efflux pump genes (*BCAL1674-BCAL1675*), due to sequence homology between the vector and target genome (Hamad et al., 2010). As before, pDAISce-I was introduced resulting in the replacement of BCAL1674-1675 by *pal*. The correct replacement was confirmed by PCR amplification. For virulence studies, the *pal* gene was also complemented using a plasmid constitutively expressing wild-type K56-2 *pal* which was constructed by amplifying the gene (primers in Table 2). Amplicons were digested with NdeI and XbaI and cloned into a similarly digested pDA12 vector, resulting in pDA12-*pal*. These complements are designated Δ*pal*(pDA-12*pal*).

G. mellonella survival assay

Log growing bacteria were diluted to OD_{600} 0.1 in sterile PBS and serially diluted to 10^{-7}. Each dilution (20 µl) was injected into the hindmost left proleg of *G. mellonella* larvae using a sterile Terumo 0.3 ml syringe (10 larvae per group). An equal volume of each dilution was also plated onto LB agar and plates were counted at 48 h to accurately quantify bioburden injected. Ten larvae injected with PBS alone served as controls. Larvae were incubated at 37 °C and examined for survival at 24, 48 and 72 h. The % larval survival was plotted against the colony forming units (CFU)

inoculated value to calculate the LD_{50} value for each strain (Costello et al., 2011). Cell-free supernatants of K56-2 wild-type and mutants were also assessed by centrifuging overnight cultures at 2,500 *g* for ten min. The supernatants were decanted into a sterile universal and filter-sterilised using a 0.20 μm filter to obtain cell-free supernatant. Aliquots (20 μl) of each supernatant were injected into groups of larvae and 20 μl of supernatant was also plated onto LB agar to ensure sterility. Ten larvae injected with LB broth alone, served as controls. In separate experiments, recombinant purified endotoxin free Pal was also injected into groups of larvae and compared with negative control and with LPS. Larval survival was examined at 24, 48 and 72 h post-inoculation and % survival relative to LB control group determined each time point.

Accumulation of fluorescent dye H33342

Cellular permeability was determined by uptake of fluorescent dye H33342 as previously described (Coldham et al., 2010). Overnight cultures were used to inoculate fresh medium and cultured for a further 5 h at 37 ^{o}C. The cells were centrifuged at 4000 g and resuspended in 1 ml PBS and OD_{600nm} adjusted to 0.1, before transferring to 96-well plates. Strains were aliquoted in replicates of eight with 8 control replicates (PBS only) and the plate transferred to a BioTek Synergy H1 Hybrid reader and incubated at 37 ^{o}C. H33342 (100 μM) was added to each well to give a final concentration of 10 μM. This optimal concentration was determined in preliminary optimisation studies comparing the fluorescence discrimination between Δ*pal* mutant and wild-type at 2.5, 10 and 100 μM H33342. Plates incubated for 90 min with fluorescent readings taken every minute (λex = 355 nm, λem = 460 nm). Raw fluorescence values were analysed by determining the mean of 8 replicates,

subtraction of the relevant control fluorescence at each time point and zero time point fluorescence to normalise for starting fluorescent value.

Cloning and expression of Pal_{Bc}

The forward primer was designed to contain the CACC sequence at the beginning of the primer to introduce a 5' overhang allowing directional cloning of the BCAL3204 (*pal*) gene into pET100/D-Topo (Thermo Fisher, Paisley, UK) (in-frame with a 35-amino acid tag construct containing the N-terminal 6xHis tag and Xpress epitope. PCR amplification was carried out using HotStar Taq polymerase (Qiagen) and amplicons cloned into the pET100/D-Topo according to the manufacturer's protocol. The TOPO® cloning reaction was added to a vial of One Shot® TOP10 Chemically Competent *E. coli* and cells heat-shocked for 30 sec at 42°C without shaking. Each transformation reaction was spread on to pre-warmed selective plates containing 50 μg/ml of ampicillin and incubated overnight at 37°C. Positive transformants were identified using PCR. BL21 Star™ (DE3) One Shot® cells were used for protein expression. After confirming Pal_{Bc} expression in a pilot study, 1 L cultures of BL21 cells transformed with the expression plasmid were grown in LB broth with ampicillin (100 μg/ml) and expression induced with IPTG at a final concentration of 1 mM for 3 h at 37 °C. Bacteria were then pelleted using centrifugation at 2,500 *g* for 10 min. Supernatants were discarded, pellets weighed and stored at -80 °C.

Pal_{Bc} purification

Purification of Pal_{Bc} was carried out as described by Franken et al. (Franken et al., 2000) with some modifications to ensure complete removal of lipopolysaccharide from the preparation. Ice-cold lysis buffer containing 6 M Guanidine-HCL, 100 mM

sodium phosphate, 10 mM Tris-HCl (pH 8) and 1X EDTA-free protease inhibitor was added to bacterial pellets at a volume of 30 ml corresponding to 7 g of wet cell pellet. Cells were resuspended in lysis buffer by vortexing and pipetting and subsequently lysed on ice with a cell disruptor using maximum output for two 30-sec pulses. Cell debris and any remaining intact cells were pelleted using centrifugation at 6,300 rpm for 35 min. Supernatants were filtered through a 0.45 µM filter and incubated with a rotating Ni-NTA column, which was pre-equilibrated with buffer A, for 1 h at 4 °C. Unbound protein and endotoxin were removed from the column by a series of washes with 8 M Urea in phosphate buffer, followed by two rounds of organic washes (60% isopropanol in 10 mM Tris HCl) alternating with 10 mM Tris HCl. Bound protein was subsequently eluted with 1 % trifluoroacetic acid followed by two additional elution steps in 250 and 300 mM imidazole. After purification, the protein concentration of each fraction was determined using the Bradford assay. Protein purity was determined by sodium dodecyl sulphate-polyacrylamide gel electrophoresis (SDS-PAGE). Proteins were concentrated using Amicon® filters with a 3 kDa cut-off, resuspended in 50 mM Tris (pH 7) and tested for endotoxin content by the *Limulus amebocyte* lysate (LAL) assay using the ToxinSensor Gel clot endotoxin assay kit (Genscript, New Jersey) according to the manufacturer's instructions. The mass of the intact purified protein was confirmed by Electron spray Mass Spectroscopy (Alta Biosciences, Birmingham, UK).

Cloning, expression and purification of truncated $Pal_{51\text{-}170}$

Bioinformatic analyses were carried out using SignalP, LipoP, XtalPred (Jahandideh et al., 2014, Bendtsen et al., 2004). Based on these analyses, the variant with the highest crystallization success rate was a Pal protein lacking the first 50 N-terminal

amino acids (Pal_{51-170}). A DNA fragment encoding Pal_{51-170} was obtained by PCR amplification (primers shown in Table 2). The amplicon was subcloned into the pETM13 expression system to obtain a C-terminal 6xHis-tag recombinant protein and introduced into *E. coli* BL21(DE3) by transformation. Overnight cultures were inoculated in 1 L LB supplemented with kanamycin (50 µg/ml), and incubated at 37°C with 180 rpm shaking until the OD_{600nm} reached 0.65. Optimal Pal_{51-170} expression was obtained using 0.8 mM isopropyl β-D-1-thiogalactopyranoside (IPTG) at 22°C for 16 h. Harvested bacterial cells were resuspended in lysis buffer (50 mM Tris-HCl, 300 mM NaCl, 5% Glycerol, 0.01% CHAPS, 10 mM Imidazole, pH 7.5) supplemented with a protease-inhibitor cocktail (Roche Diagnostic). After sonication and subsequent centrifugation at 30,000 *g* for 30 min, the soluble fraction was purified by affinity chromatography using a 5 mL Ni-NTA column (GE Healthcare). After washing with Binding Buffer (50 mM Tris-HCl, 300 mM NaCl, 5% Glycerol, 0.01% CHAPS, pH 7.5), Pal_{51-170} was eluted with a linear gradient of Imidazole (5-300 mM) and the fraction collected was analysed by SDS-PAGE. A final purification step by size exclusion chromatography was performed using S75 10/300 (GE Healthcare) column in 50 mM Tris-HCl, 150 mM NaCl, 5% Glycerol, pH 7.5. The eluted fractions were concentrated using Amicon ultra column (Millipore) at a final concentration of 30 mg/ml for crystallization experiments, resulting in a protein of 14894.1 Da as calculated by mass spectrometry.

Extraction and analysis of LPS

Stationary-phase cultures (500 ml) of K56-2 wild-type and Δ*pal* mutant strains were centrifuged at 4,000 rpm for 10 min to pellet bacteria and each pellet weighed. Pellets were then washed with endotoxin-free water, pelleted again and resuspended in 10 ml

of endotoxin-free water. Bacteria were disrupted by sonication in ice-cold water for 10 min. Bacterial lysates and a 90% phenol solution were equilibrated at 65 °C before the addition of 10 ml of the phenol solution to the lysates (Davis and Goldberg, 2012) for a further 50 min at 65 °C with regular vigorous shaking. Lysates were subsequently incubated on ice for 20 min before centrifugation at 2,500 *g* for 25 min at 4 °C to separate aqueous and phenol fractions. The aqueous layer was carefully removed and placed in a fresh 50 ml tube. The phenol layer was placed back in the 65 °C water bath and 10 ml of water pre-heated to 65 °C was added. Tubes were incubated for a further 30 min with vigorous shaking as before, cooled and centrifuged and the aqueous layer retained. Aqueous fractions, containing LPS, were placed in pre-equilibrated dialysis tubing (3.5 kDa cut-off) and tubing placed in 2 L beakers containing ultrapure water. Dialysis was carried out at 4 °C over 4 days, with water changed twice daily, to ensure the complete removal of phenol. Dialysed fractions were placed into separate round-bottomed flasks and lyophilised overnight. Lyophilised crude LPS was removed carefully from round-bottomed flasks, placed into sterile tubes and weighed. LPS extracts were resuspended in endotoxin-free water to a final concentration of 1 mg/ml. LPS from both strains was analysed on 15 % acrylamide gels.

Effect of purified Pal and LPS on G. mellonella survival

Purified endotoxin-free Pal_{Bc} was reconstituted in 50mM Tris buffer (400µg/ml) and a range concentrations (12.5 to 150µg/ml) were injected into groups of larvae (10 larvae per group) in an injection volume of 20µl. Larvae were injected with 50 mM Tris buffer alone or either 150 and 1000µg/ml LPS as controls. Aliquots of 20 µl of

each purified protein and LPS were also plated onto LB-agar for 48 hours to determine if there was any bacterial contamination.

Attachment of bacteria to epithelial cells

To quantify the attachment of either *B. cenocepacia* or Pal_{Bc}-expressing *E. coli* strains to lung epithelial cells, CFBE41o$^-$ cells were seeded in coated chamber slides 24 h prior to the 30 min incubation of individual bacterial strains at an MOI of 50:1, as previously described (McClean et al., 2016). In the experiments with recombinant *E. coli* strains, expression was induced with 1 mM IPTG for 3 h prior to incubation with epithelial cells. Unattached bacteria were removed by washing with sterile PBS four times for five min each. Attachment was quantified by lysing the cells with 0.5% Triton X for 20 min, scraping the cells to remove them, serially diluting in PBS and plating on LB agar plates. Plates were incubated at 37 °C and CFU were counted after 48 h. Attachment was also confirmed by confocal microscopy after fixing the CFBE41o$^-$ cells in 3 % paraformaldehyde (pH 7.2) for 10 min at room temperature. Cells were gently washed once with PBS and then blocked in PBS containing 5% bovine serum albumin for one hour at room temperature. Cells were incubated overnight at 4 °C in PBS containing 1 % bovine serum albumin and either rabbit anti-Bcc (1:800 dilution) or FITC-conjugated anti-*E. coli* antibodies (1:100 dilution). In the case of *B. cenocepacia* strains, the next day cells were washed three times with PBS before the addition of FITC-conjugated anti-rabbit antibody (1:500 dilution) for one hour in the dark. The secondary antibody was removed and cells washed twice for five min each with PBS. Cells were then counterstained with DAPI and phalloidin conjugated to Alexa fluor 568 (5U/ ml) for 15 min in the dark at a concentration of 1 μg/ml in PBS to highlight the nuclei and intracellular area via staining of actin

filaments with the cytoplasm, respectively. A coverslip was applied to each chamber before bacteria and cells were visualised using confocal microscopy. Bacterial attachment was counted in 20 randomly selected fields for each strain, in three independent experiments and values were expressed as the number of bacteria/100 cells.

Cytokine analysis

CFBE41o$^-$ cells were seeded overnight in antibiotic-free medium in 24-well plates at a density of 4 x 10^5 cells/well and subsequently the medium was replaced with antibiotic free and serum-free medium, and cells incubated overnight. The next day bacteria were incubated with CFBE 41o$^-$ cells at an MOI of 50:1 at 37 °C in 5 % CO_2 environment for 24 h. Alternatively, CFBE41o$^-$ cells were incubated with Pal_{Bc} protein (10-100 µg/ml) for 24 h, purified LPS from K56-2 (100 µg) or MEM alone; the latter two served as positive and negative controls, respectively. The next day, plates were centrifuged at 1,500 *g* for 10 min and supernatants retained and stored at -80 °C. Cytokine analysis was performed using the MesoScaleDiscovery (MSD, Gaithersburg, MD, USA, www.mesoscale.com) Multispot system. For this, cell supernatants were diluted 1 in 5 with MEM and then an equal volume of Diluent was added. The 4-plex multi-array electrochemiluminescence platform (detection range 0.008 ng/ml to 1000 ng/ml, i.e. factor 125000) was used to measure ten cytokines (IFNγ, IL-10, IL12p70, IL-13, IL-1β, IL-2, IL-4, IL-6, IL-8, TNFα) simultaneously in cell supernatants. This system uses multi-array plates fitted with multi-electrodes per well with each electrode being coated with a different capture antibody. Each sample was analyzed in duplicate on the same array plate. Samples and calibrator solutions were added to plates coated with cytokine-specific capture antibodies and incubated

overnight at 4 °C before washing 3 times with 100 µl of PBS containing 0.05 % Tween-20. The nine detection antibodies (120 µl each) were combined at a final volume of 6 ml; 25 µl of the mixture were added to each well and incubated with the plate for 1 h. Wells were washed three times with PBS containing 0.05 % Tween-20 (100 µl), before reading on the MSD plate reader.

Circular Dichroism spectroscopy

Circular dichroism measurements were carried out using a Jasco J-810 spectropolarimeter equipped with a Peltier temperature control system (Model PTC-423-S). The molar ellipticity per mean residue, $[\theta]$(deg cm^2 x $dmol^{-1}$), was calculated from the equation $[\theta] = [\theta]obs \times mrw \times (10 \times l \times C)^{-1}$, where $[\theta]obs$ is the ellipticity measured in degrees, mrw is the mean residue molecular mass (105.3 Da), C is the protein concentration in g x l^{-1} and l is the optical path length of the cell in centimetres. Far-UV spectra (190–260 nm) of Pal_{51-170} were recorded at 293K using a 0.1 cm optical path-length cell, with a protein concentration of 0.2 mg/ml. For thermal denaturation experiments, ellipticity was monitored at 222 nm with a temperature slope of 1°C/min from 20°C to 100°C. Melting temperature was calculated from the maximum of the first derivative of the unfolding curves.

Sequence conservation analysis

Sequence conservation analysis was carried out using ConSurf (Goldenberg et al., 2009). The homologue search algorithm CSI-BLAST was used to retrieve sequences from the UNIREF-90 sequence database using an E-value cut-off of 0.001. Sequences were aligned using MAFFT-L-INS-I alignment method (Katoh and Standley, 2013).

Light Scattering Analysis

Purified Pal_{51-170} was analyzed by size exclusion chromatography coupled with light scattering using a DAWN MALS instrument and an Optilab rEX (Wyatt Technology). Eight hundred micrograms of purified Pal_{51-170} were loaded into a S75 16/60 column (GE Healthcare), equilibrated in 50 mM Tris-HCl, 150 mM NaCl, 5% Glycerol, pH 7.5. The on-line measurement of the intensity of the Rayleigh scattering as a function of the angle, as well as the differential refractive index of the eluting peak in size exclusion chromatography, was used to determine the weight average molar mass (Mw) of eluted protein, using the Astra 5.3.4.14 (Wyatt Technologies) software.

Isothermal Titration Calorimetry

ITC experiments were performed at 295 K using a high-sensitive titration calorimeter system (MicroCal iTC200, Malvern, UK) with a reference power of 8 cal/s and a stirring speed of 1000 rpm. To remove endogenous peptidoglycan fragments, purified Pal_{51-170} was extensively dialyzed in a denaturing buffer (4 M GuHCl, 25 mM Tris-HCl and 150 mM NaCl, pH 7.5) at room temperature for 16 h and then refolded in 25 mM Tris-HCl, 200 mM NaCl and 0.005 % (v/v) CHAPS, pH 7.5) for 3-4 days. Ligand sample was dissolved in the dialysis buffer. For the ITC measurements, the dipeptide iE-DAP was purchased from InvivoGen (San Diego, CA, USA). Titration experiments consisted of additions of 19 injections with 2 μL of ligand (2 mM) to the protein solution contained in the cell (0.27 mL of 0.1 mM of Pal_{51-170}) with 150-s equilibration between injections. Data were analyzed with Origin 5.0 software (MicroCal) with a single-site model.

Crystallization of Pal_{51-170}.

Crystallization trials were performed using hanging drop vapour diffusion technique at 293K. Preliminary crystallization trials were performed using a robot station (Hamilton STARlet NanoJet 8+1) for high throughput crystallization screening with commercially available sparse matrix kits (Crystal Screen kit I e II, Index, PEG/ION, Hampton Research). Optimization of crystallization conditions was performed manually using the additive Hampton screening. The best crystals were obtained at a protein concentration of 30 mg/ml in 0.1M bis[2-Hydroxyethyl]imino-tris[hydroxymethyl]methane pH 5.5, 25% w/v Polyethylene glycol 3350, 10 mM $MgCl_2$. Cryoprotection of the crystals was achieved by a fast soaking in a solution containing glycerol to a final concentration of 25% (v/v). The data sets were scaled and merged using HKL2000 program package. Statistics of data collection are reported in Table 3. The crystal structure was solved by Molecular Replacement using the software Phaser (McCoy et al., 2007), and the structure of acute phase antigen BPSL2765 from *B. pseudomallei* as a template (Gourlay et al., 2013). Crystallographic refinement was first carried out against 95% of the measured data using the CCP4 program suite (Potterton et al., 2003). The remaining 5% of the observed data, which were randomly selected, was used in Rfree calculations to monitor the progress of refinement. The structure was validated using PROCHECK (Laskowski et al., 1996). Coordinates and structure factors were deposited with the Protein Data Bank with the PDB code 5LKW.

Analysis of Lipid A

Overnight cultures in 100 ml of LB were washed twice with phosphate buffer (pH 7.4) and freeze dried. Lipid A was extracted by resuspending lyophilized bacterial

cells (10 mg) in a mixture of isobutyric acid:1 M ammonium hydroxide (400 µl, 5:3, v/v) and heating at 100°C for 2 h with vortexing every 15 min, and then centrifuged at 2000 *g* for 15 min. The supernatant was mixed with an equal volume of water and lyophilized. The sample was washed with methanol twice and lipid A was solubilized in 80 µl of chloroform:methanol:water (3:1.5:0.25, v/v, 80 µl) for 4 h. Lipid A suspension was desalted with grains of ion-exchange resin (Dowex 50W-X8; H+). Desalted lipid A suspension (2 µl) was loaded on polished steel target, air dried and covered with 1 µl of 2,5-dihydroxybenzoic acid matrix (Sigma Chemical Col, St. Louis, MO) dissolved in 0.1 M citric acid aqueous solution and allowed to dry. The target was inserted in a Bruker Autoflex MALDI-TOF spectrometer. Data acquisition and analysis were performed using the Flex Analysis software.

Statistical analysis

Statistical analysis of cytokine release and Bcc attachment to epithelial cells was carried out using one-way ANOVA followed by Bartlett's test, using GraphPad Prism. Comparison of attachment of *E. coli* BL21 Star cells expressing or not expressing Bc Pal was performed by one-way ANOVA using Minitab software. Comparison of the fluorescent dye accumulation curves was performed by two-way ANOVA using GraphPad Prism. Log-Rank test of survival data were performed using the GraphPad Prism software version 6.0 (GraphPad Software, San Diego California) ****P<0.001.

Acknowledgements

We are most grateful to Dr Dieter Gruenert (UCSF) for the gift of CFBE41o$^-$ cells and Dr Umadevi Sajjan (University of Michigan) for the gift of the anti-Bcc antibody. This research was supported by grant SFI 11/RFP.1/BMT/3307 from the Science Foundation Ireland (to SMcC) and EU COST Action BM1003: "Microbial cell surface determinants of virulence as targets for new therapeutics in cystic fibrosis for Short Term Scientific Missions" (to SMcC, MAV, and RB).

Conflict of Interest.

The authors have no conflicts of interest to declare.

References.

Bendtsen, J. D., Nielsen, H., Von Heijne, G. and Brunak, S. (2004). Improved prediction of signal peptides: SignalP 3.0. *J Mol Biol,* **340**: 783-95.

Berenson, C. S., Murphy, T. F., Wrona, C. T. and Sethi, S. (2005). Outer membrane protein P6 of nontypeable Haemophilus influenzae is a potent and selective inducer of human macrophage proinflammatory cytokines. *Infect Immun,* **73**: 2728-35.

Blair, D. F., Kim, D. Y. and Berg, H. C. (1991). Mutant MotB proteins in Escherichia coli. *J Bacteriol,* **173**: 4049-55.

Cascales, E., Bernadac, A., Gavioli, M., Lazzaroni, J. C. and Lloubes, R. (2002). Pal lipoprotein of Escherichia coli plays a major role in outer membrane integrity. *J Bacteriol,* **184**: 754-9.

Coldham, N. G., Webber, M., Woodward, M. J. and Piddock, L. J. (2010). A 96-well plate fluorescence assay for assessment of cellular permeability and active efflux in Salmonella enterica serovar Typhimurium and Escherichia coli. *J Antimicrob Chemother,* **65**: 1655-63.

Costello, A., Herbert, G., Fabunmi, L., Schaffer, K., Kavanagh, K. A., Caraher, E. M., *et al.* (2011). Virulence of an emerging respiratory pathogen, genus Pandoraea, in vivo and its interactions with lung epithelial cells. *J Med Microbiol,* **60**: 289-99.

Davis, M. R., Jr. and Goldberg, J. B. (2012). Purification and visualization of lipopolysaccharide from Gram-negative bacteria by hot aqueous-phenol extraction. *J Vis Exp*.

De Mot, R. and Vanderleyden, J. (1994). The C-terminal sequence conservation between OmpA-related outer membrane proteins and MotB suggests a common function in both gram-positive and gram-negative bacteria, possibly in the interaction of these domains with peptidoglycan. *Mol Microbiol,* **12**: 333-4.

De Smet, B., Mayo, M., Peeters, C., Zlosnik, J. E., Spilker, T., Hird, T. J., *et al.* (2015). Burkholderia stagnalis sp. nov. and Burkholderia territorii sp. nov., two novel Burkholderia cepacia complex species from environmental and human sources. *Int J Syst Evol Microbiol,* **65**: 2265-71.

De Vries, S. P. W., Eleveld, M. J., Hermans, P. W. M. and Bootsma, H. J. (2013). Characterization of the Molecular Interplay between <italic>Moraxella catarrhalis</italic> and Human Respiratory Tract Epithelial Cells. *PLoS One,* **8**: e72193.

Drevinek, P. and Mahenthiralingam, E. (2010). Burkholderia cenocepacia in cystic fibrosis: epidemiology and molecular mechanisms of virulence. *Clin Microbiol Infect,* **16**: 821-30.

Elsner, A., Kreikemeyer, B., Braun-Kiewnick, A., Spellerberg, B., Buttaro, B. A. and Podbielski, A. (2002). Involvement of Lsp, a member of the LraI-lipoprotein family in Streptococcus pyogenes, in eukaryotic cell adhesion and internalization. *Infect Immun,* **70**: 4859-69.

Figurski, D. H. and Helinski, D. R. (1979). Replication of an origin-containing derivative of plasmid RK2 dependent on a plasmid function provided in trans. *Proc Natl Acad Sci U S A,* **76**: 1648-52.

Flannagan, R. S., Linn, T. and Valvano, M. A. (2008). A system for the construction of targeted unmarked gene deletions in the genus Burkholderia. *Environ Microbiol,* **10**: 1652-60.

Franken, K. L., Hiemstra, H. S., Van Meijgaarden, K. E., Subronto, Y., Den Hartigh, J., Ottenhoff, T. H. and Drijfhout, J. W. (2000). Purification of his-tagged proteins by immobilized chelate affinity chromatography: the benefits from the use of organic solvent. *Protein Expr Purif,* **18**: 95-9.

Gaspar, J. A., Thomas, J. A., Marolda, C. L. and Valvano, M. A. (2000). Surface expression of O-specific lipopolysaccharide in Escherichia coli requires the function of the TolA protein. *Mol Microbiol,* **38**: 262-75.

Gerding, M. A., Ogata, Y., Pecora, N. D., Niki, H. and De Boer, P. A. (2007). The trans-envelope Tol-Pal complex is part of the cell division machinery and required for proper outer-membrane invagination during cell constriction in E. coli. *Mol Microbiol,* **63**: 1008-25.

Godlewska, R., Wisniewska, K., Pietras, Z. and Jagusztyn-Krynicka, E. K. (2009). Peptidoglycan-associated lipoprotein (Pal) of Gram-negative bacteria: function, structure, role in pathogenesis and potential application in immunoprophylaxis. *FEMS Microbiol Lett,* **298**: 1-11.

Goldenberg, O., Erez, E., Nimrod, G. and Ben-Tal, N. (2009). The ConSurf-DB: pre-calculated evolutionary conservation profiles of protein structures. *Nucleic Acids Res,* **37**: D323-7.

Gourlay, L. J., Peri, C., Ferrer-Navarro, M., Conchillo-Sole, O., Gori, A., Rinchai, D., *et al.* (2013). Exploiting the Burkholderia pseudomallei acute phase antigen BPSL2765 for structure-based epitope discovery/design in structural vaccinology. *Chem Biol,* **20**: 1147-56.

Gray, A. N., Egan, A. J., Van't Veer, I. L., Verheul, J., Colavin, A., Koumoutsi, A., *et al.* (2015). Coordination of peptidoglycan synthesis and outer membrane constriction during Escherichia coli cell division. *Elife,* **4**.

Hamad, M. A., Di Lorenzo, F., Molinaro, A. and Valvano, M. A. (2012). Aminoarabinose is essential for lipopolysaccharide export and intrinsic

antimicrobial peptide resistance in Burkholderia cenocepacia(dagger). *Mol Microbiol,* **85**: 962-74.

Hamad, M. A., Skeldon, A. M. and Valvano, M. A. (2010). Construction of aminoglycoside-sensitive Burkholderia cenocepacia strains for use in studies of intracellular bacteria with the gentamicin protection assay. *Appl Environ Microbiol,* **76**: 3170-6.

Hanuszkiewicz, A., Pittock, P., Humphries, F., Moll, H., Rosales, A. R., Molinaro, A., *et al.* (2014). Identification of the flagellin glycosylation system in Burkholderia cenocepacia and the contribution of glycosylated flagellin to evasion of human innate immune responses. *J Biol Chem,* **289**: 19231-44.

Hellman, J., Roberts, J. D., Jr., Tehan, M. M., Allaire, J. E. and Warren, H. S. (2002). Bacterial peptidoglycan-associated lipoprotein is released into the bloodstream in gram-negative sepsis and causes inflammation and death in mice. *J Biol Chem,* **277**: 14274-80.

Henry, D. A., Campbell, M. E., Lipuma, J. J. and Speert, D. P. (1997). Identification of Burkholderia cepacia isolates from patients with cystic fibrosis and use of a simple new selective medium. *J Clin Microbiol,* **35**: 614-9.

Isles, A., Maclusky, I., Corey, M., Gold, R., Prober, C., Fleming, P. and Levison, H. (1984). Pseudomonas cepacia infection in cystic fibrosis: an emerging problem. *J Pediatr,* **104**: 206-10.

Jahandideh, S., Jaroszewski, L. and Godzik, A. (2014). Improving the chances of successful protein structure determination with a random forest classifier. *Acta Crystallogr D Biol Crystallogr,* **70**: 627-35.

Katoh, K. and Standley, D. M. (2013). MAFFT multiple sequence alignment software version 7: improvements in performance and usability. *Mol Biol Evol,* **30**: 772-80.

Kaza, S. K., Mcclean, S. and Callaghan, M. (2010). IL-8 released from human lung epithelial cells induced by cystic fibrosis pathogens Burkholderia cepacia complex affects the growth and intracellular survival of bacteria. *Int J Med Microbiol,* **301**: 26-33.

Kim, K., Kim, K. P., Choi, J., Lim, J. A., Lee, J., Hwang, S. and Ryu, S. (2010). Outer membrane proteins A (OmpA) and X (OmpX) are essential for basolateral invasion of Cronobacter sakazakii. *Appl Environ Microbiol,* **76**: 5188-98.

Kovacs-Simon, A., Titball, R. W. and Michell, S. L. (2011). Lipoproteins of bacterial pathogens. *Infect Immun,* **79**: 548-61.

Laskowski, R. A., Rullmannn, J. A., Macarthur, M. W., Kaptein, R. and Thornton, J. M. (1996). AQUA and PROCHECK-NMR: programs for checking the quality of protein structures solved by NMR. *J Biomol NMR,* **8**: 477-86.

Lazzaroni, J. C., Germon, P., Ray, M. C. and Vianney, A. (1999). The Tol proteins of Escherichia coli and their involvement in the uptake of biomolecules and outer membrane stability. *FEMS Microbiol Lett,* **177**: 191-7.

Liang, M. D., Bagchi, A., Warren, H. S., Tehan, M. M., Trigilio, J. A., Beasley-Topliffe, L. K., *et al.* (2005). Bacterial peptidoglycan-associated lipoprotein: a naturally occurring toll-like receptor 2 agonist that is shed into serum and has synergy with lipopolysaccharide. *J Infect Dis,* **191**: 939-48.

Makidon, P. E., Knowlton, J., Groom, J. V., 2nd, Blanco, L. P., Lipuma, J. J., Bielinska, A. U. and Baker, J. R., Jr. (2010). Induction of immune response to the 17 kDa OMPA Burkholderia cenocepacia polypeptide and protection against

pulmonary infection in mice after nasal vaccination with an OMP nanoemulsion-based vaccine. *Med Microbiol Immunol,* **199**: 81-92.

Mcclean, S. (2012). Eight stranded beta-barrel and related outer membrane proteins: Role in bacterial pathogenesis. *Protein Pept Lett*.

Mcclean, S., Healy, M. E., Collins, C., Carberry, S., O'shaughnessy, L., Dennehy, R.*, et al.* (2016). Linocin and OmpW are involved in attachment of the cystic fibrosis associated pathogen Burkholderia cepacia complex to lung epithelial cells and protect mice against infection. *Infect Immun*.

Mccoy, A. J., Grosse-Kunstleve, R. W., Adams, P. D., Winn, M. D., Storoni, L. C. and Read, R. J. (2007). Phaser crystallographic software. *J Appl Crystallogr,* **40**: 658-674.

Michel, L. V., Shaw, J., Macpherson, V., Barnard, D., Bettinger, J., D'arcy, B.*, et al.* (2015). Dual Orientation of the Outer Membrane Lipoprotein Pal in Escherichia coli. *Microbiology*.

Michel, L. V., Snyder, J., Schmidt, R., Milillo, J., Grimaldi, K., Kalmeta, B.*, et al.* (2013). Dual orientation of the outer membrane lipoprotein P6 of nontypeable haemophilus influenzae. *J Bacteriol,* **195**: 3252-9.

Miller, V. L. and Mekalanos, J. J. (1988). A novel suicide vector and its use in construction of insertion mutations: osmoregulation of outer membrane proteins and virulence determinants in Vibrio cholerae requires toxR. *J Bacteriol,* **170**: 2575-83.

O'grady, E. P. and Sokol, P. A. (2011). Burkholderia cenocepacia differential gene expression during host-pathogen interactions and adaptation to the host environment. *Front Cell Infect Microbiol,* **1**: 15.

Ortega, X., Hunt, T. A., Loutet, S., Vinion-Dubiel, A. D., Datta, A., Choudhury, B.*, et al.* (2005). Reconstitution of O-specific lipopolysaccharide expression in Burkholderia cenocepacia strain J2315, which is associated with transmissible infections in patients with cystic fibrosis. *J Bacteriol,* **187**: 1324-33.

Park, J. S., Lee, W. C., Yeo, K. J., Ryu, K. S., Kumarasiri, M., Hesek, D.*, et al.* (2012). Mechanism of anchoring of OmpA protein to the cell wall peptidoglycan of the gram-negative bacterial outer membrane. *FASEB journal : official publication of the Federation of American Societies for Experimental Biology,* **26**: 219-28.

Parsons, L. M., Lin, F. and Orban, J. (2006). Peptidoglycan recognition by Pal, an outer membrane lipoprotein. *Biochemistry,* **45**: 2122-8.

Peeters, C., Zlosnik, J. E., Spilker, T., Hird, T. J., Lipuma, J. J. and Vandamme, P. (2013). Burkholderia pseudomultivorans sp. nov., a novel Burkholderia cepacia complex species from human respiratory samples and the rhizosphere. *Syst Appl Microbiol,* **36**: 483-9.

Plesa, M., Kholti, A., Vermis, K., Vandamme, P., Panagea, S., Winstanley, C. and Cornelis, P. (2004). Conservation of the opcL gene encoding the peptidoglycan-associated outer-membrane lipoprotein among representatives of the Burkholderia cepacia complex. *J Med Microbiol,* **53**: 389-98.

Potterton, E., Briggs, P., Turkenburg, M. and Dodson, E. (2003). A graphical user interface to the CCP4 program suite. *Acta Crystallogr D Biol Crystallogr,* **59**: 1131-7.

Prasadarao, N. V., Wass, C. A., Weiser, J. N., Stins, M. F., Huang, S. H. and Kim, K. S. (1996). Outer membrane protein A of Escherichia coli contributes to invasion of brain microvascular endothelial cells. *Infect Immun,* **64**: 146-53.

Rodriguez-Herva, J. J., Ramos-Gonzalez, M. I. and Ramos, J. L. (1996). The Pseudomonas putida peptidoglycan-associated outer membrane lipoprotein is involved in maintenance of the integrity of the cell cell envelope. *J Bacteriol,* **178**: 1699-706.

Seed, K. D. and Dennis, J. J. (2008). Development of Galleria mellonella as an alternative infection model for the Burkholderia cepacia complex. *Infect Immun,* **76**: 1267-75.

Shinoy, M., Dennehy, R., Coleman, L., Carberry, S., Schaffer, K., Callaghan, M.*, et al.* (2013). Immunoproteomic analysis of proteins expressed by two related pathogens, Burkholderia multivorans and Burkholderia cenocepacia, during human infection. *PLoS One,* **8**: e80796.

Spinola, S. M., Wild, L. M., Apicella, M. A., Gaspari, A. A. and Campagnari, A. A. (1994). Experimental human infection with Haemophilus ducreyi. *J Infect Dis,* **169**: 1146-50.

Sukumaran, S. K., Shimada, H. and Prasadarao, N. V. (2003). Entry and intracellular replication of Escherichia coli K1 in macrophages require expression of outer membrane protein A. *Infect Immun,* **71**: 5951-61.

Torres, A. G. and Kaper, J. B. (2003). Multiple elements controlling adherence of enterohemorrhagic Escherichia coli O157:H7 to HeLa cells. *Infect Immun,* **71**: 4985-95.

Verhoeven, G. S., Dogterom, M. and Den Blaauwen, T. (2013). Absence of long-range diffusion of OmpA in E. coli is not caused by its peptidoglycan binding domain. *BMC microbiology,* **13**: 66.

Vines, E. D., Marolda, C. L., Balachandran, A. and Valvano, M. A. (2005). Defective O-antigen polymerization in tolA and pal mutants of Escherichia coli in response to extracytoplasmic stress. *J Bacteriol,* **187**: 3359-68.

Winther, T., Xu, L., Berg-Sorensen, K., Brown, S. and Oddershede, L. B. (2009). Effect of energy metabolism on protein motility in the bacterial outer membrane. *Biophysical journal,* **97**: 1305-12.

Zhu, X., Bagchi, A., Zhao, H., Kirschning, C. J., Hajjar, R. J., Chao, W.*, et al.* (2007). Toll-like receptor 2 activation by bacterial peptidoglycan-associated lipoprotein activates cardiomyocyte inflammation and contractile dysfunction. *Crit Care Med,* **35**: 886-92.

Table 1: Strains and plasmids used in this study

Strain or plasmid	Characteristics	Origin
B. cenocepacia		
K56-2 (LMG18863)	ET12 clone related to J2315, cystic fibrosis isolate	BCRRC, CF clinical isolate
Δ*pal*	Deletion of *pal* (BCAL3204) in K56-2	This study
Δ*pal*(*pal*$^{+}$)	Chromosomal *pal* integration in K56-2 Δ*pal*	This study
Δ*pal(pDA-12pal)*	Plasmid complemented on pDA-12 plasmid	This study
E. coli		
NCIB9485	Strain B/r	Laboratory collection
GT115	F^{-} *mcr*A Δ(*mrr-hsd*RMS-*mcrBC*) Φ80Δ*lac*ZΔM15 Δ*lac*X74 *recA1 rpsL* (StrA) *endA1*Δ*dcm uidA* (ΔMIuI*)::pir-116* Δ*sbcC-sbcD*	Invitrogen
SY327	*araD* Δ(*lac pro*) *argE*(Am) *recA*56 *nalA* λ*pir*; Rif^{R}	(Miller and Mekalanos, 1988)
DH5α	F^{-} ϕ80dlacZΔM15 Δ(*lacZYA-argF*)U169 *endA*1 *recA*1 *hsdR*17(rK^{-} mK^{+}) *supE*44 *thi*-1 Δ*gyrA*96 *relA*1	Laboratory collection
Top10	F^{-} *mcr*A Δ(*mrr-hsd*RMS-*mcr*BC) Φ80*lac*ZΔM15 Δ*lac*X74 *rec*A1 *ara*D139 Δ(*ara-leu*)7697 *gal*U *gal*K *rps*L (Str^{R}) *end*A1 *nup*G	Invitrogen
BL21 Star^{TM} (DE3)	F^{-} *ompT hsdS*B (rB^{-}mB^{-}) *gal dcm rne131* (DE3)	Invitrogen
Plasmids		
pGPIScel-2	*ori*$_{R6K}$, ΩTp^{R} , mob^{+}, containing the ISce-I restriction site	(Flannagan et al., 2008)
pRK2013	*ori*$_{ColE1}$, RK2 derivative, Kan^{R}, mob^{+}, tra^{+}	(Figurski and Helinski, 1979)
pDAI-SceI	Encodes the ISce-I homing endonuclease, Tet^{R}	(Flannagan et al., 2008)
pMH447	pGPI-SceI derivative used for chromosomal complementation	(Hamad et al., 2012)
pDA12	*ori*$_{pBBR1}$, Tet^{R}, *mob*$^{+}$, P$_{dhfr}$ used for plasmid complementation	(Aubert 2008)
pET100/D-Topo	Peptide fusion at N-terminal, 6xHis, Amp^{R}	Invitrogen

Table 2. Primers used in this study

Region:	5'-3' primer sequence:	Product size (bp)	Restriction enzymes:
Upstream	actgacgaattctggcggtgcgccacagatcta tgatataagcttattgtttgccttgtcgtcgag	513	EcoRI HindIII
Downstream	tcaattaagcttgaagccgtgagcctcggcaa agtgatgctagcctctgcggatacttcgcgatg	612	HindIII NheI
Complementation	ttttcatatgatgtcgaataaagctcgt gttttctagattactgttggtagacgag	533	NdeI XbaI
Internal	ttcggtgaaggacgagtacc cacggcttccatttgagaat	205	N/A
Cloning	caccatgatgtcgaataaagct cgttacttactgttggtagac	526	N/A
Pal_{51-170}	catgccatgggcgtcgatccgctgaacgacc gatgctcgagctgttggtagacgaggtcg	382	N/A

Table 3. Structural data collection and refinement statistics. Values in parentheses are for the highest resolution shells 2.15-2.00 Å.

Data collection	**Apo**
Space group	$P3_2$
Unit-cell parameters *a, b, c* (Å), γ (°)	77.7, 77.7, 38.6, 120
Resolution range (Å)	30.0-2.0
Wavelength (Å)	1.542
Mosaicity (°)	0.5
Average redundancy	5.5 (5.4)
Unique reflections	14094
Completeness (%)	100.0 (100.0)
†R_{merge} (%)	8.4 (43.8)
Average I/σ(I)	4.9 (3.2)

Refinement	
Resolution range (Å)	15.0-2.0
Rwork/Rfree (%)	19.4/24.2
No. of residues	240
No. of water molecules	176
R.m.s. deviations	
Bond lengths (Å)	0.01
Bond angles (°)	1.5

†R_{merge}= Σ hΣi |$I(h,i)$-<$I(h)$>|/ Σ hΣi $I(h,i)$, where $I(h,i)$ is the intensity of the ith measurement of reflection h and <$I(h)$> is the mean value of the intensity of reflection h.

Figure Legends

Fig. 1. Pal plays a role in bacterial membrane integrity.

A. Genetic organization of the gene cluster encoding Pal and Tol proteins in *B. cenocepacia* J2315 and K56-2. Grey arrows indicate the direction of transcription of each gene. BCAL gene designations are according to annotation of the *B. cenocepacia* J2315 genome (http://www.sanger.ac.uk/Projects/B _cenocepacia/).

B. Survival of *G. mellonella* after 72 h exposure to supernatants from K56-2 wild-type (●) and Δ*pal* mutant (■) and complemented strain Δ*pal*(*pal*$^{+}$) (▲). * P<0.0001, Log Rank (Mantel-Cox) test comparison between the virulence of K56-2 wild-type and Δ*pal* mutant.

C. Effect of Pal on membrane permeability. Accumulation of H33342 fluorescent dye was examined in the Δpal mutant, complement and wild type K56-2 cells over 90 minutes.

Fig. 2. Pal does not affect LPS structure but is involved in polymyxin resistance.

A. Effect of Pal on LPS structure. Extracted LPS from K56-2 wild-type and the Δ*pal* mutant strain. Lane 1: wild-type LPS. Lane 2: Δ*pal* mutant LPS. Samples were run on a 15 % acrylamide gel and stained with silver stain.

B. Mass spectrometry of lipid A from wild-type K56-2 and the Δ*pal* mutant. Lipid A was extracted from bacteria, desalted with ion-exchange resin, loaded on polished steel target, with 1 μl of 2,5-dihydroxybenzoic acid matrix before analysis on a MALDI-TOF mass spectrometer. Data acquisition and analysis were performed using the Flex Analysis software.

Fig. 3. Pal is a lipoprotein with a stable α-β conformation**.**

A. Domain organization of Pal_{Bc} according to the Pfam database. The signal peptide (SP) and cleavage site were predicted by Signal P 4.1 and LipoP 1.0 servers, respectively.

B. Gel filtration profile of Pal_{51-170} along with the SDS PAGE analysis of main fractions. Pal_{51-170} was eluted from a Ni NTA column with an Imidazole gradient and fractions collected were analysed by SDS PAGE.

C. Size exclusion chromatography-multi angle light scattering analysis; the grey curve represents the Rayleigh ratio (left scale) against the elution time. Molecular mass values (Mw, right scale), corresponding to a monomeric state, are reported in black.

D. CD spectrum of Pal_{51-170} measured on a spectropolarimeter equipped with a Peltier temperature control system. Molar ellipticity per mean residue was calculated in the far UV range at 293 K with a protein concentration of 0.2 mg/ml.

E. Thermal denaturation of Pal_{51-170} achieved by following the CD signal at 222 nm as a function of temperature.

Fig. 4. Structural determination of Pal_{51-170}

A. Ribbon representation of Pal_{51-170} crystal structure (chain A). The α helices and β strands are marked.

B. Molecular surface of Pal_{51-170} (green) highlighting the cavity; Arg-120 is coloured blue.

C. Degree of residue conservation on the protein surface (Consurf analysis). Residue coloring, reflecting the degree of residue conservation, ranges from magenta (highly

conserved) to cyan (variable). The most conserved residues lining the cavity are labelled.

D. Omit (Fo-Fc) electron density map contoured at 2.0 σ of the DAP moiety in the cavity. H-bonding interactions are indicated with dashed lines.

Fig. 5. Isothermal titration calorimetry confirmed that Pal_{51-170} can bind to DAP.

A. Raw data for the titration of Pal_{51-170} with iE-DAP (inset). Binding isotherms were measured at pH7.5 and showed exothermic heats of binding that decreased with each successive injection of iE-DAP up to a point of saturation.

B. Integrated heats of binding obtained from the raw data, after subtracting the heat of dilution. The solid line represents the best curve fit to the experimental data, using the single site model from MicroCal Origin.

Fig. 6. Pal_{Bc} stimulates cytokine secretion from CF epithelial cells.

Cytokine secretion was measured after exposure of CFBE41o- cells to wild-type K56-2, Δ*pal* mutant strain or Pal_{Bc}, as determined by multi-array electrochemi-luminescence.

A and B. IL-8 (A) and IL-6 (B) secretion from CFBE41o- cells after incubation with wild-type K56-2, Δ*pal* mutant, purified LPS or medium alone. Error bars represent the standard deviation of three independent biological repeats, ***$p<0.001$ relative to wild-type.

C and D. IL-8 (C) and IL-6 (D) secretion in response to increasing concentrations of Pal_{Bc} (10-100 μg/ml) compared to LPS (100 μg/ml) or medium alone (control). Error bars represent the standard deviation of three independent biological repeats. *$p<0.05$, **$p<0.01$, ***$p<0.001$ relative to the medium-only control

Fig. 7. Pal_{Bc} is involved in CF epithelial cell attachment.

A. Attachment of K56-2, Δ*pal* mutant and *E. coli* NCIB 9485 control strain to CFBE41o$^-$ cells determined by CFU/ml after incubation of epithelial cells with the strains at an MOI 50:1. Error bars represent the standard error of the mean (SEM) from 4 independent experiments. * $p<0.05$, compared with the attachment of K56-2 wild-type.

B. Confocal microscopy images confirming the attachment of wild-type, Δ*pal* mutant and Δ*pal*(*pal*$^+$)complemented strains to CFBE41o$^-$ cells. Bacteria were labelled using a primary anti-Bcc antibody and detected with a secondary FITC-conjugated polyclonal antibody (green). CFBE41o$^-$ cells were counterstained with DAPI (blue). *$P<0.05$. C. Quantification of attachment from confocal microscopy. Graph represents *B. cenocepacia* attachment to CFBE41o$^-$ cells, using an MOI 50:1. Data represents the number of bacteria/100 cells for each strain. Error bars represent the standard error of the mean (SEM) from 3 independent experiments. *$P<0.05$

Fig. 8. *E. coli* expressing Pal_{Bc} showed increased attachment over E. coli wild type.

A. Representative confocal microscopy images representing the attachment of *E. coli* BL21 control and *E. coli* BL21(pET100/D-Topo) strain expressing Pal_{Bc} to CFBE41o$^-$ cells. Bacteria were labelled using a FITC-conjugated primary anti-*E. coli* antibody (green). Nuclei of CFBE41o$^-$ cells were counterstained with DAPI (blue) and actin stained with phalloidin conjugated with Alexa fluor 568.

B. Quantitation of the attachment of *E. coli* BL21 control and *E. coli* BL21(pET100/D-Topo) strain expressing Pal_{Bc} attachment to CFBE41o$^-$ cells, using an MOI 50:1. Data represents the mean number of bacteria/ 100 cells for each strain

determined by counting 20 individual fields per strain in each of three experiments. Error bars represent the standard error of the mean (SEM) from three independent experiments, *P<0.0001.

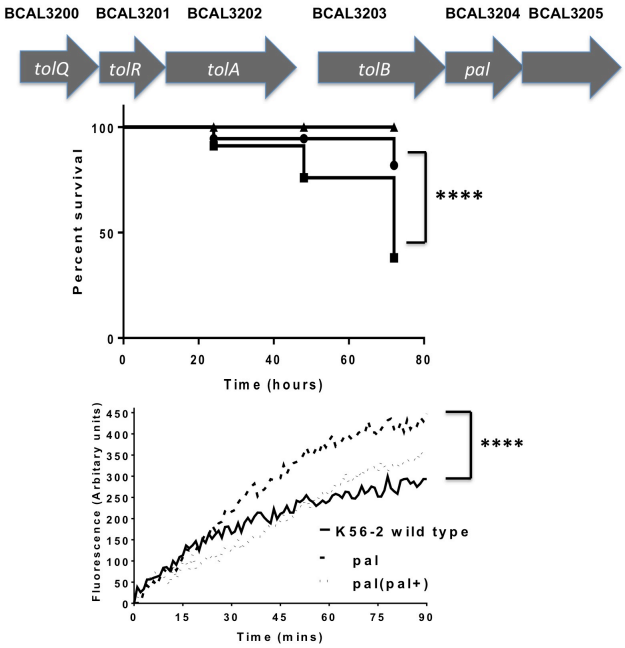
BCAL3200
BCAL3201
BCAL3202
BCAL3203
BCAL3204
BCAL3205
tolQ
tolR
tolA
tolB
pal
Percent survival
100
50
0
0
20
40
60
80
Time (hours)
****
Fluorescence (Arbitary units)
450
400
350
300
250
200
150
100
50
0
0
15
30
45
60
75
90
Time (mins)
K56-2 wild type
pal
pal(pal+)
****

Figure 1

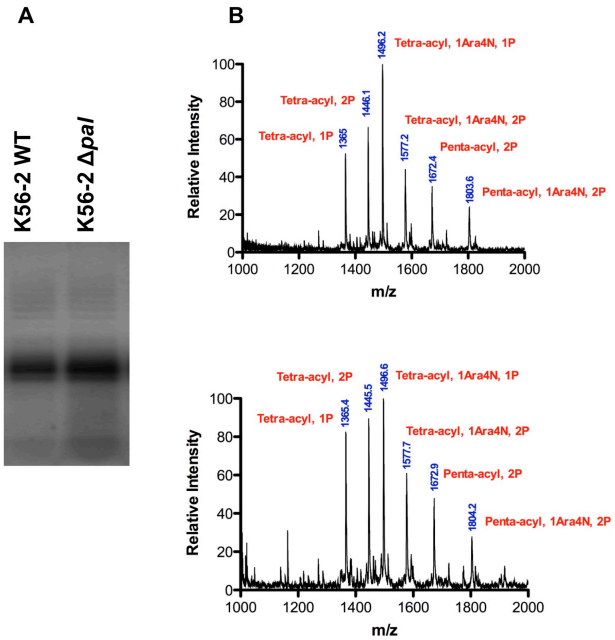

Figure 2:

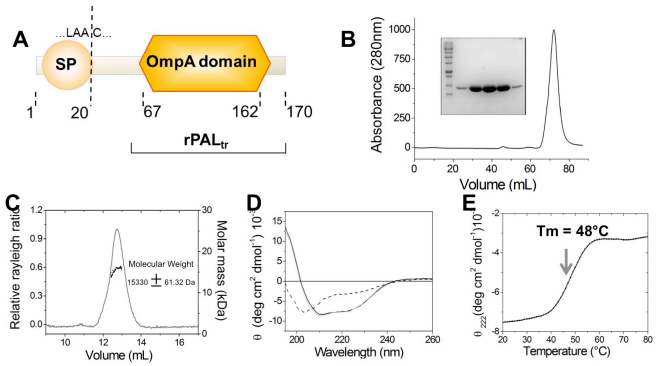

Figure 3

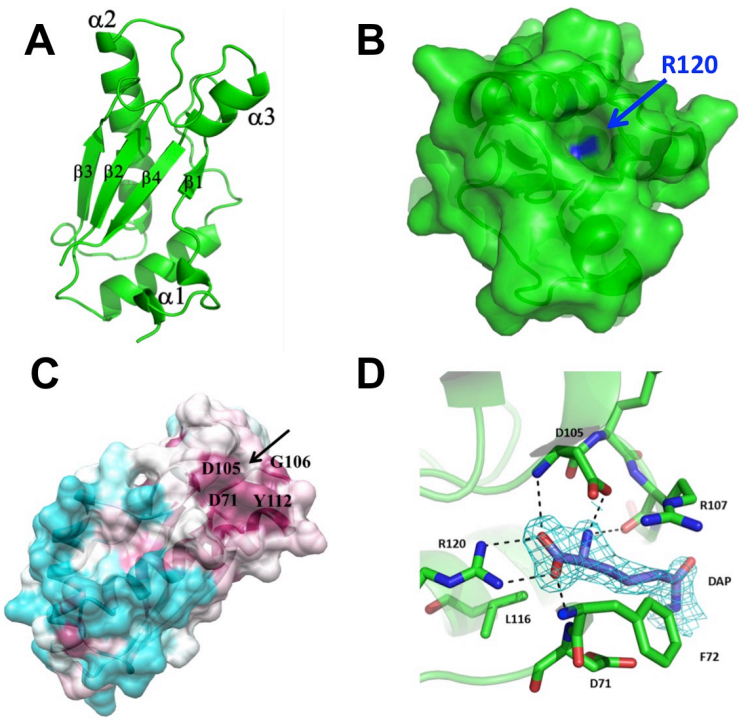

Figure 4

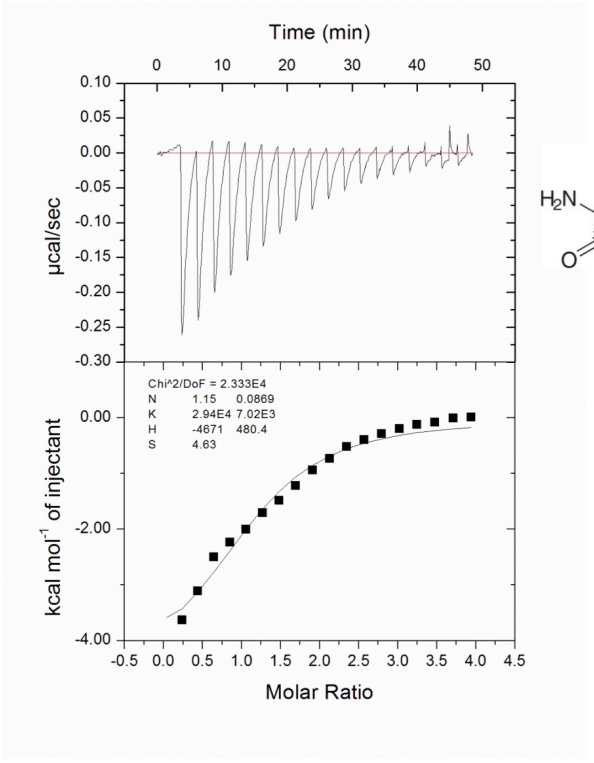

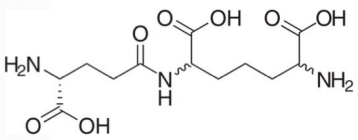

iE-DAP

Fig 5

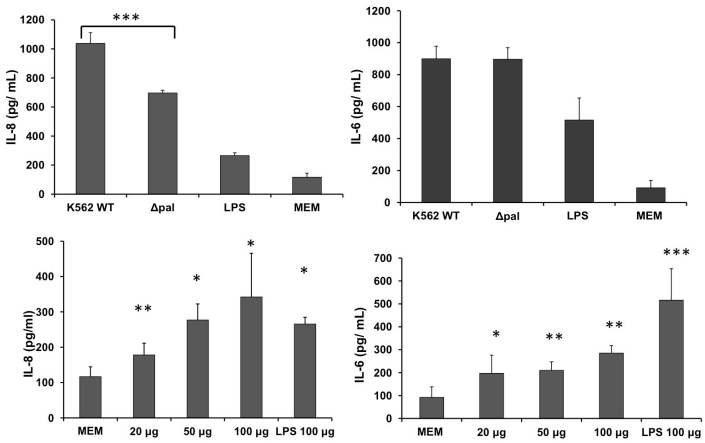

Figure 6

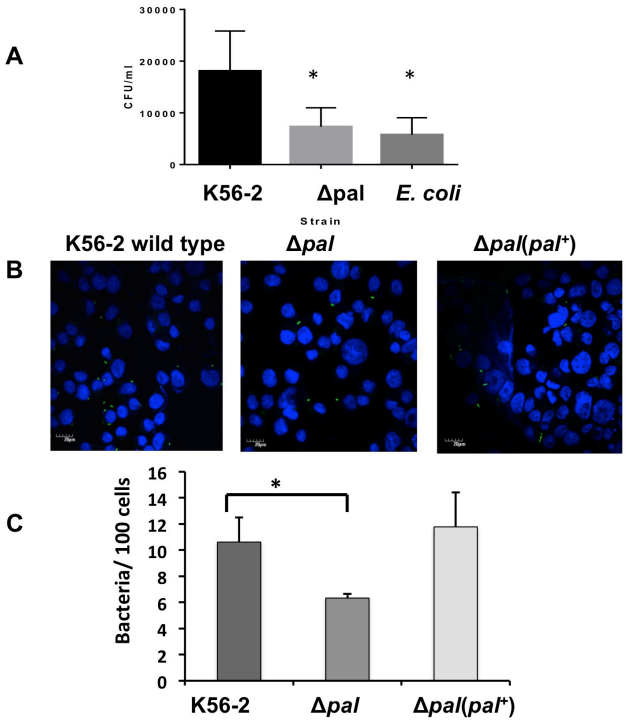

Figure 7

Figure 8

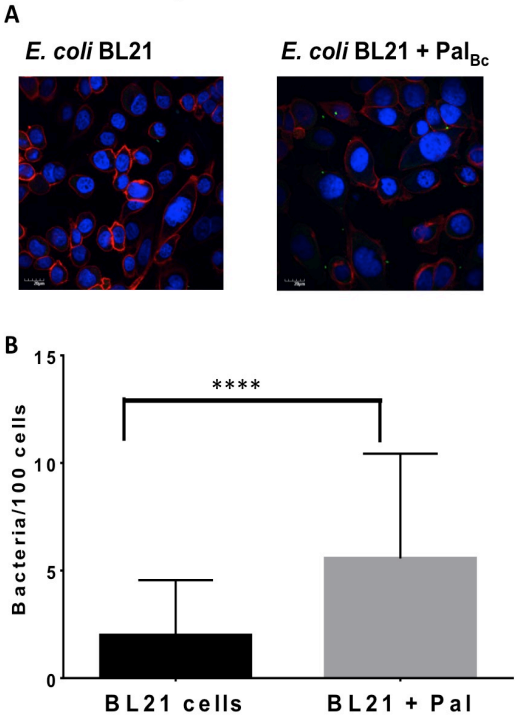
A
E. coli BL21
E. coli BL21 + Pal$_{Bc}$
B
Bacteria/100 cells
15
10
5
0
****
BL21 cells
BL21 + Pal

Supplementary figures:

Fig. S1

Polymyxin B and meropenem sensitivities of wild-type K 56-2, Δpal mutant and Δpal(pal+) strains as determined by E-test strips (polymyxin 0.064-1.024µg/ml; meropenem 0.002=31µg/ml. Images are representative of three independent experiments.

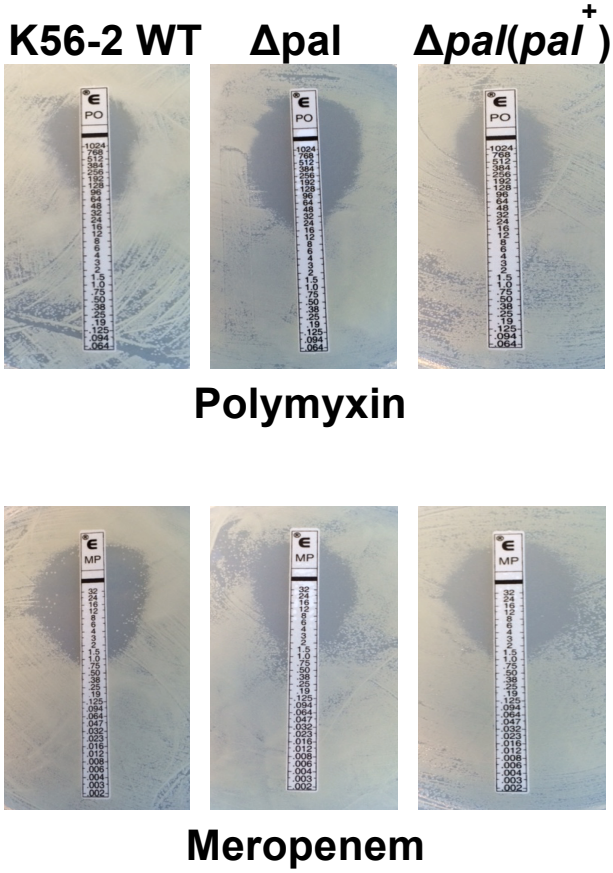

Fig. S2 : Expressed Pal_{Bc} highlighting polyHis tag, Xpress epitope, signal peptide and lipobox.

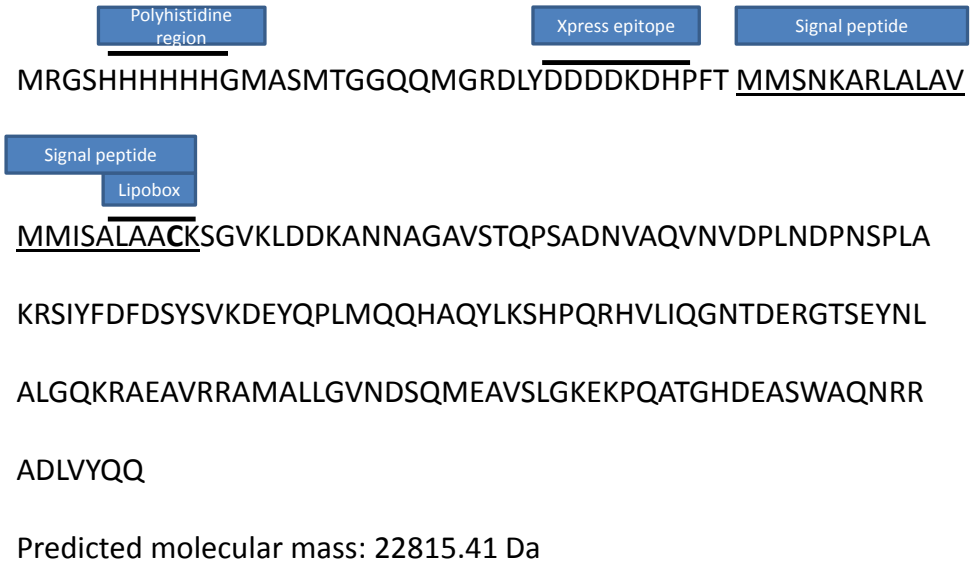

Predicted molecular mass: 22815.41 Da

Fig. S3: Pal_{Bc} identified as a palmitoylated, dimyristated and dilaurylated forms and in unacylated form.

	Expected mass (+/- 5da)	**Observed mass**
PAL_{Bc} (with His-tag and Xpress epitope)	22815.41	22820.0
DAP residue	190.2	Not found
+DAP + dilaurylate	23412.04	23408.0
+DAP + dimyristate	23467.54	23460.0
+DAP + dipalmitate	23520.22	23520.0

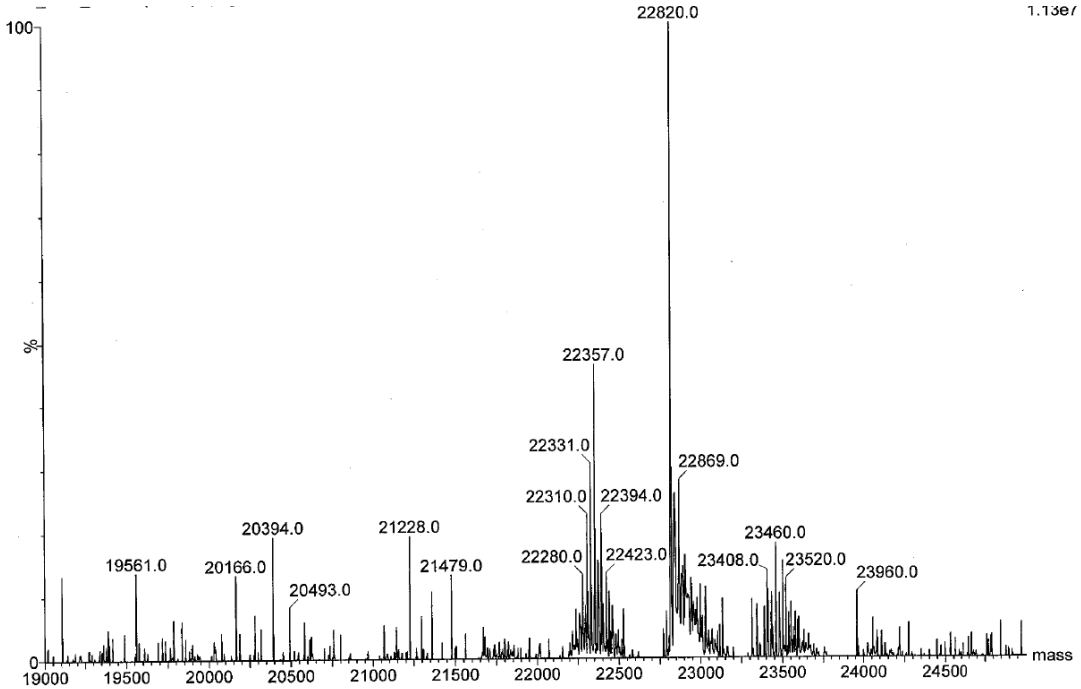

Fig. S4. DAP incorporation into the cavity of Pal_{51-170}.

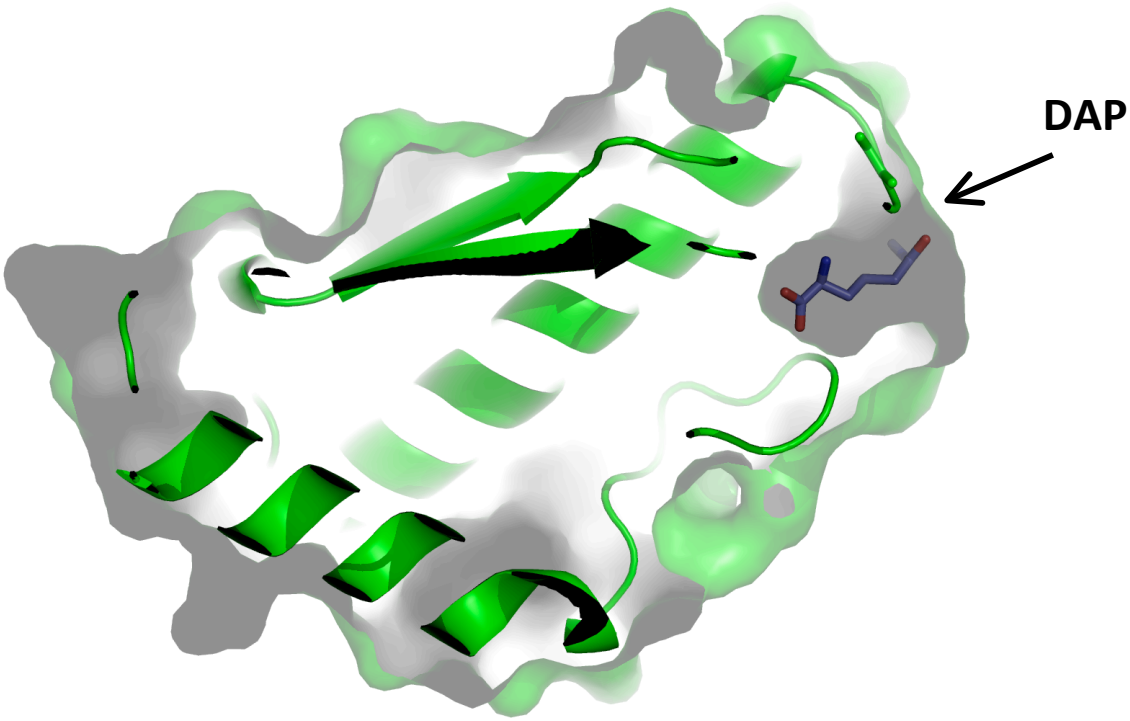

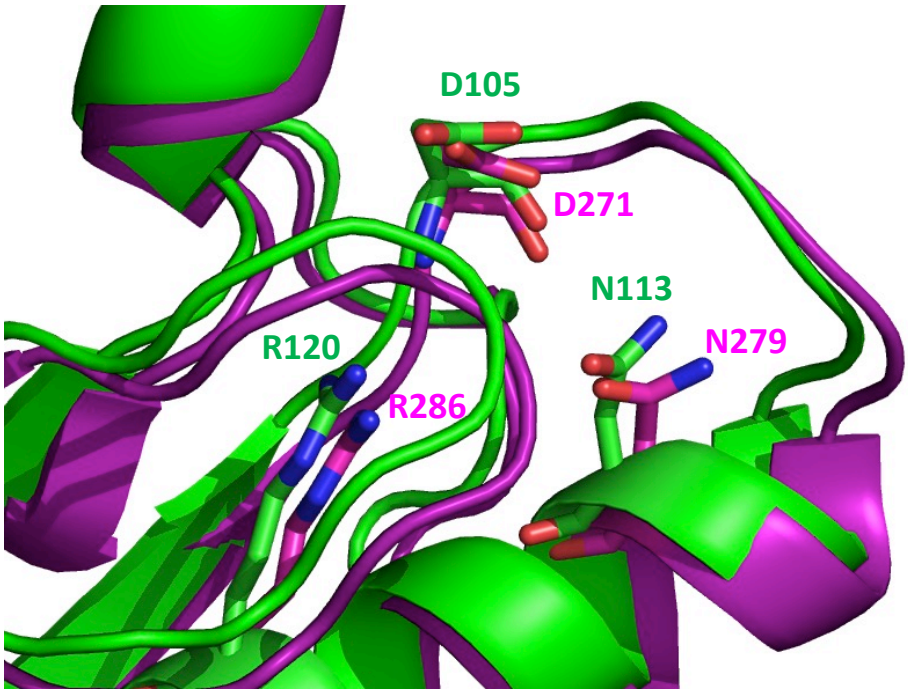

Fig. S5. Structural organization of the residues interaction with Pal_{51-170}